

# Peel Adhesion and Viscoelasticity of Poly(ethylene-co-vinyl acetate)-Based Hot Melt Adhesives. I. The Effect of Tackifier Compatibility

H.-H. SHIH\* and G. R. HAMED

Department of Polymer Science, University of Akron, Akron, Ohio

## SYNOPSIS

A series of poly(ethylene-co-vinyl acetate) (EVA)-based hot melt adhesives containing either a rosin or a hydrocarbon (C5-C9) tackifier have been prepared to investigate viscoelastic properties and peel adhesion. Fracture energies were determined by the use of a T-Peel geometry (two polypropylene films bonded with model EVA adhesives). The rosin has only one glass transition temperature, but the C5-C9 resin has two glass transition temperatures, indicating phase separation. The rosin has better compatibility with EVA than does the C5-C9 resin. The bond strength of tackified EVA to polypropylene depends not only on compatibility, but also on viscoelastic properties. A higher storage modulus results in a higher T-Peel strength. Under certain test conditions, glassy C5-C9-rich domains act as reinforcing filler, resulting in a higher storage modulus. Here, a C5-C9-tackified EVA adhesive has higher T-Peel strength than does one containing rosin. © 1997 John Wiley & Sons, Inc.

## INTRODUCTION

Hot melt adhesives (HMAs) spread onto substrates in the melt followed by solidification after cooling. Thermoplastics, such as poly(ethylene-co-vinyl acetate) (EVA), polyolefins, polyamides, and polyesters, have been the basis of HMAs. A typical EVA-based HMA is formulated with four main components: polymer, tackifier, wax, and antioxidant. The polymer contributes strength and toughness, while the tackifier enhances wetting and tack. The wax lowers melt viscosity and reduces cost. The antioxidant reduces thermal degradation during processing. EVA-based hot melt adhesives are widely used in packaging, paper laminating, nonwoven textiles, and book bindings.<sup>1</sup>

The influence of tackifier on the viscoelasticity and peel adhesion of elastomers has been studied by many authors.<sup>2</sup> Tackifier addition increases

the glass transition temperature and the storage modulus at a high strain rate, while lowering the storage modulus at low strain rates. Tackifier also acts as a diluent to lower the entanglement density, resulting in a decreased plateau modulus.

Tackifiers often have limited compatibility with rubber. Phase separation, which can be inferred from viscoelastic measurements or observed by electron microscopy, often is found in tackified rubber. One phase contains elastomer saturated with resin, and the other contains resin saturated with elastomer.<sup>3</sup> The miscibility between tackifier and elastomer depends on the resin structure, the molecular weight of the resin, and the resin concentration.<sup>4-6</sup>

Although tackifiers are widely used in formulating EVA-based HMA, few scientific investigations have been concerned with HMA. In one study,<sup>7</sup> the peel force, determined only at one testing condition, was found to increase with increasing tackifier/EVA compatibility. One purpose of this study was to determine whether this holds at other testing conditions. In another study,<sup>8</sup> using higher testing temperatures, EVA compositions with 45 wt % resin and 10 wt % wax had higher

\* To whom correspondence should be addressed.

T-Peel strength than did the corresponding composition with only resin. The reverse was true at a low testing temperature. It is unclear why there is a crossover.

Dynamic mechanical thermal analysis (DMTA) was used to discern tackifier compatibility with EVA. The T-Peel fracture energies of polypropylene (PP)/HMA/PP laminates were measured. Finally, compatibility-viscoelasticity-peel adhesion relationships are discussed.

## EXPERIMENTAL: MATERIALS AND SPECIMENS PREPARATION

Two tackifiers were used; one is an aliphatic-aromatic hydrocarbon resin (C5-C9; Escorez 2393, Exxon Company), and the other is a hydrogenated rosin ester (rosin, Foral 105; Hercules Company). Raw materials, including EVA (Escorene 7750; Exxon Company), the two tackifiers, and wax, were combined to give a total batch weight of 45 g. Compositions were melt blended at 120°C for 6 min in a Haake mixer. To reduce thermal degradation, 0.25 parts by weight of antioxidant (Irganox 165; Ciba Geigy Company) was added. Mixtures were compression molded at 120°C for 10 min under 20 tons of force to form sheets 1.5 mm thick.

Samples are designated as E-T (X : Y), where E and T represented EVA and tackifier, respectively; X : Y is the ratio of EVA to tackifier. Detailed sample designations and formulations are listed in Table I.

Differential scanning calorimetry (DSC), with a sample size of about 10 mg, was used to measure the glass transition temperature of the rosin and C5-C9. Temperature was increased from room temperature to 100°C at 10°C/min. Then, samples

were quenched to room temperature and rerun from -50 to 150°C at 10°C/min.

Strips about 5 mm wide were cut, and a Dynamic Mechanical Thermal Analyzer was used to measure  $E'$  and the glass transition temperatures of model adhesives. The temperature range was -50 to 50°C at an increasing rate of 2°C/min; the frequency was 1 Hz. In order to determine the two glass transition temperatures of a heterogeneous blend,  $\tan \delta$  curves were decomposed by the following methodology. A function representing the  $\tan \delta$  curve is written as

$$F(T) = A_L \exp(-(T - T_{g-L})^2/B_L) + A_H \exp(-(T - T_{g-H})^2/B_H) \quad (1)$$

where  $A_L$  and  $A_H$  are the peak heights of peaks corresponding to the EVA- and rosin-rich phases, respectively;  $B_L$  and  $B_H$  are equal to 1.2 times the temperature width at the half-height position of the corresponding peak;  $T$  is the temperature; and  $T_{g-L}$  and  $T_{g-H}$  are the peak temperatures of the peaks corresponding to the EVA- and rosin-rich phases, respectively. First, two numbers representing the two peak temperatures were given and substituted into eq. (1). Then,  $A_L$ ,  $A_H$ ,  $B_L$ , and  $B_H$  were adjusted until the minimum standard error deviation for this pair was reached. Another pair of temperatures was given, and  $A_L$ ,  $A_H$ ,  $B_L$ , and  $B_H$  were obtained again. This trial-and-error was continued, until the smallest standard error deviation was obtained. Thus, the two temperatures giving the best curve fit were assigned as the two glass transition temperatures of the heterogeneous blend. The peak heights also were recorded.

Samples of E-R (5 : 5), E-5 (8 : 2), E-5 (7 : 3), and E-5 (5 : 5) which are 1.5 mm thick were cut into 3 mm × 1 mm strips. These were cooled to -70°C in the ultramicrotome and sliced at a gauge setting of 70 nm. Samples were transferred onto nickel screens. Samples were stained with OsO<sub>4</sub> vapor (4 wt % water solution) for 72 h at room temperature and were coated with carbon. Morphologies were observed by the use of transmission electron microscopy (TEM; JEM-1200 EX II, Japan Electron Optics Laboratory).

An adhesive layer (0.23 mm thick) and a 0.16 mm brass spacer were placed between two sheets of polypropylene (0.13 × 200 × 50 mm). The sandwich was placed between two chrome plates and pressed at 120°C and a 3,400 kg/m<sup>2</sup> load for 100 sec with a hot sealer (Sencorp System Inc.). After

**Table I Formulations (Parts by Weight)**

Sample	Components			
	EVA	Rosin	C5-C9	Antioxidant
EVA	100			
E-R (8 : 2)	80	20		0.25
E-R (7 : 3)	70	30		0.25
E-R (5 : 5)	50	50		0.25
E-R (4 : 6)	40	60		0.25
E-5 (8 : 2)	80		20	0.25
E-5 (7 : 3)	70		30	0.25
E-5 (5 : 5)	50		50	0.25

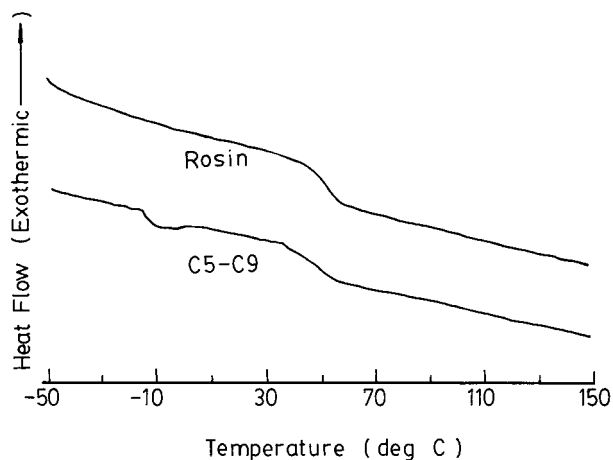


**Figure 1** DSC thermogram of rosin and C5-C9 resin.

bonding, the tapes were cooled in air to room temperature. The total thickness of the specimens was  $0.42 \pm 0.02$  mm (with an adhesive thickness of  $0.16 \pm 0.02$  mm). Strips, 25 mm wide and 175 mm long (including 150 mm of bonded PP/HMA/PP and 25 mm of free PP film on one side), were cut for testing. The bond strengths of the laminates were determined in a T-Peel geometry at three temperatures (11, 21, and 31°C) and five rates (5, 20, 50, 200, and 500 mm/min) with an Instron. Peeling energy was determined from the peeling force by the following equation:

$$G = 2F/b \quad (2)$$

where  $G$  is the peeling energy (N/m);  $F$  is the average force required to peel a specimen apart (N); and  $b$  is the width of the test specimen (m). Stick- and slip-band lengths were measured with a traveling microscope. The fractions of stick and slip in a stick-slip cycle also were calculated.

## RESULTS AND DISCUSSION

### Glass Transition Temperatures of Tackifiers

The DSC responses of the rosin and the C5-C9 are shown in Figure 1. The materials are amorphous with no melting points. The glass transition temperature of the rosin is 52°C. C5-C9 exhibits two glass transitions (i.e., -12 and 46°C), suggesting phase separation.

### Viscoelastic Properties of Rosin/EVA Adhesives

Tan  $\delta$  versus temperature plots for E-R (8 : 2), E-R (7 : 3), E-R (5 : 5), and E-R (4 : 6) are shown

in Figure 2. The rosin and EVA are not completely compatible when the concentration is above 50 wt % rosin, but they are compatible at 30 wt % rosin or less. The glass transition temperatures of E-R (8 : 2) and E-R (7 : 3) are listed in Table 2. After decomposition of the tan  $\delta$  curves of E-R (5 : 5) and E-R (4 : 6), the glass transition temperatures of the EVA-rich ( $T_{g-L}$ ) and tackifier-rich ( $T_{g-H}$ ) phases were obtained. These are also listed in Table II.

For a single phase, the Fox equation<sup>9</sup> can be used to predict the glass transition temperature of the rosin. By the use of this equation and the tan  $\delta$  peak temperatures from Figure 2,  $T_{g, \text{rosin}}$  is calculated to be 50 and 42°C, based on the results from blends with 30 and 20 wt % of rosin, respectively. The average, 46°C, is close to the  $T_g$  found by DSC.

The storage moduli ( $E'$ ) of rosin-tackified EVA are plotted in Figure 3. For homogeneous HMAs (20 and 30 wt % rosin), the values of  $E'$  are higher than those of EVA, when temperatures are lower than their glass transitions. Above the glass transition temperatures, the  $E'$  values of E-R (8 : 2) and E-R (7 : 3) become lower than that of EVA. For E-R (5 : 5), a heterogeneous blend, the crossover temperature is located at the higher glass transition temperature, corresponding to the rosin-rich phase. A similar trend is seen for E-R (4 : 6). These findings suggest that when the temperature is higher than a specific temperature (either the  $T_g$  of a single-phase blend or the  $T_{g-H}$  of a two-phase blend), the tackifier acts a plasticizer, diminishing EVA entanglements, thereby

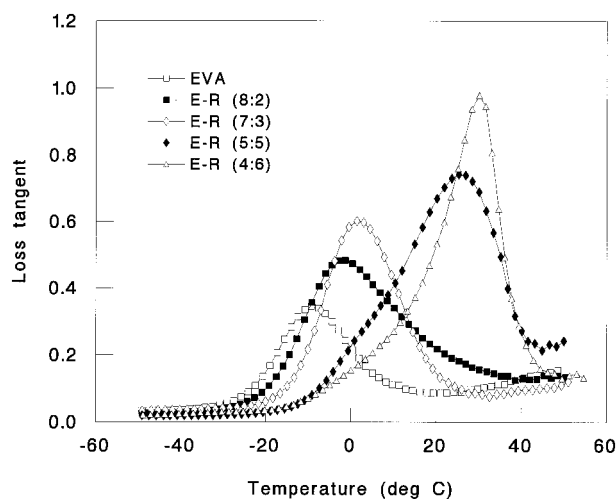


**Figure 2** Effect of rosin concentration on the loss tangent of EVA, measured by DMTA at 1 Hz and 2°C/min.

**Table II**  $\tan \delta$  Height and Width and Glass Transition Temperature of Various Rosin-Tackified EVA After Decomposition

EVA	$T_g$ ( $^{\circ}\text{C}$ )	$T_{g,L}$ ( $^{\circ}\text{C}$ )	Height	Width ( $^{\circ}\text{C}$ )	$T_{g,H}$ ( $^{\circ}\text{C}$ )	Height	Width ( $^{\circ}\text{C}$ )
E-R (8 : 2)	-1						
E-R (7 : 3)	5.5						
E-R (5 : 5)		6	0.2008	12.4	26	0.7052	14.2
E-R (4 : 6)		16	0.2942	15.0	30	0.8050	8.0

decreasing the storage modulus. As temperature falls below this critical temperature, the tackifier acts as filler and, thus, raises the storage modulus. This behavior has been found before, and an explanation has been proposed by Kraus and Hanshimoto.<sup>10</sup>

### Viscoelastic Properties of EVA/C5-C9 Adhesives

$\tan \delta$  versus temperature plots for E-5 (8 : 2), E-5 (7 : 3), and E-5 (5 : 5) are shown in Figure 4. It is quite clear that the C5-C9 resin and EVA are not compatible at a 50/50 composition. However, it is difficult to discern whether there is only one peak or two overlapping peaks at 20 and 30 wt % of C5-C9. In the DSC, the C5-C9 resin showed two transition temperatures, suggesting two phases. If both were soluble at low concentrations in EVA, this could result in one phase, with the EVA acting as a compatibilizer.

One approach is to assume that there is only one  $T_g$  for E-5 (8 : 2) and E-5 (7 : 3), at  $-3$  and  $5^{\circ}\text{C}$ , respectively. Then, the  $T_g$  of C5-C9 can be

calculated from the Fox equation. Predicted values are  $39$  and  $23^{\circ}\text{C}$ , based on compositions with  $30$  and  $20$  wt % of C5-C9 resin. These two values are quite different, suggesting that E-5 (8 : 2) and E-5 (7 : 3) are not homogeneous.

The storage moduli of C5-C9-tackified EVA are plotted in Figure 5. For EVA with  $20$  and  $30$  wt % C5-C9, crossovers are also observed. However, the crossover temperatures of E-5 (8 : 2) and E-5 (7 : 3) are located at  $6$  and  $17^{\circ}\text{C}$ , which are  $9$  and  $12^{\circ}\text{C}$  higher than the peak temperatures, respectively. This further suggests that both of the adhesives are two-phase systems.

In order to determine the glass transition temperatures of E-5 (8 : 2) and E-5 (7 : 3),  $\tan \delta$  curves were decomposed. The results are listed in Table III. The higher glass transition temperature ( $19^{\circ}\text{C}$ ) of E-5 (7 : 3) is quite close to the crossover temperature ( $17^{\circ}\text{C}$ ) found in the  $E'$  versus temperature plot. Similar results are found for E-5 (8 : 2). This strongly suggests that EVA containing  $20$  and  $30$  wt % of resin is heterogeneous. Therefore, the reasoning used to explain

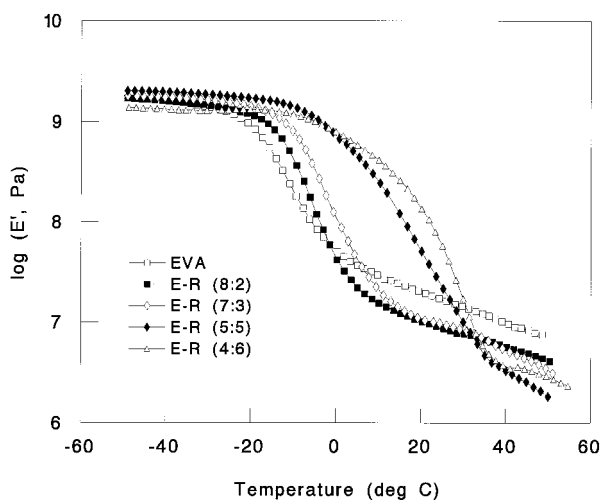


**Figure 3** Effect of rosin concentration on the storage modulus of EVA, measured by DMTA at  $1$  Hz and  $2^{\circ}\text{C}/\text{min}$ .

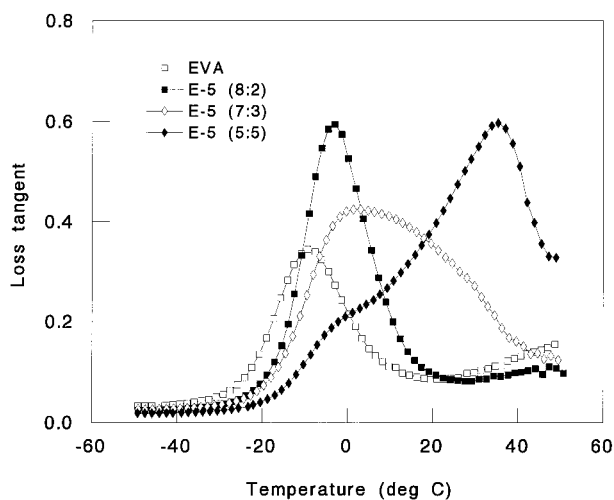


**Figure 4** Effect of C5-C9 concentration on the loss tangent of EVA, measured by DMTA at  $1$  Hz and  $2^{\circ}\text{C}/\text{min}$ .

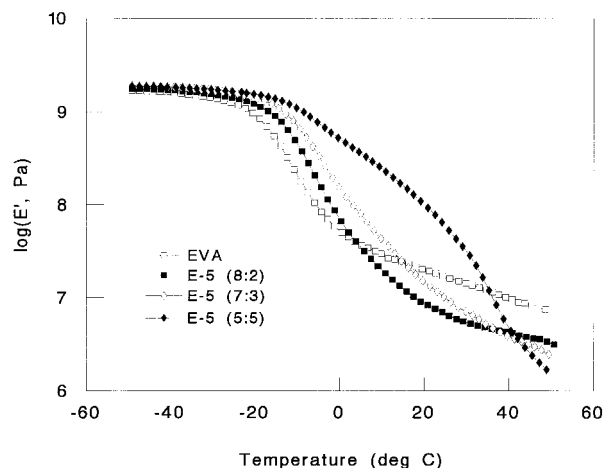


**Figure 5** Effect of C5-C9 concentration on the storage modulus of EVA, measured by DMTA at 1 Hz and 2°C/min.

the viscoelastic behavior of E-R (5 : 5) is applicable to the EVA/C5-C9 adhesives.

### Morphology Observation by TEM

Islands (lighter, white spots) and sea (slightly gray area) are noticeable for E-5 (5 : 5) (Fig. 6). Nonstained areas (EVA-rich phase) are bright white in this picture. There is some unsaturation in C5-C9, which is readily stained by OsO<sub>4</sub>, resulting in the slightly gray area.<sup>11</sup> The domain size of the EVA-rich phase is about 0.5 μm. Similar results are found for E-5 (7 : 3) (Fig. 7); however, the contrast between the two phases is poorer. The domain size of the EVA-rich phase is increased to 0.9 μm. For E-5 (8 : 2), the sea and island pattern is hard to discern (Fig. 8). This is probably due to the low concentration of the C5-C9-rich phase, which prohibits good contrast.

For E-R (5 : 5), the island and sea pattern cannot be seen clearly (Fig. 9) because of poor contrast between domains. A possible reason follows. The hydrogenated rosin has very few residual double bonds,<sup>12-14</sup> resulting in less ability to stain. Moreover, the EVA and rosin have similar

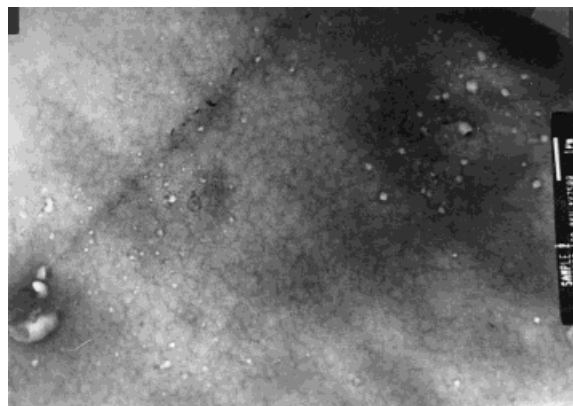


**Figure 6** Morphology observation by the use of TEM for E-5 (5 : 5).

ester functionality, which may give better compatibility between the two. The phase separation morphology of E-R (5 : 5) is hard to observe by the use of TEM, although two glass transition temperatures were found in DMTA testing.

On the basis of the TEM results, it is evident that E-5 (5 : 5) and E-5 (7 : 3) are heterogeneous. However, the contrast in the TEM picture of E-5 (8 : 2) is too poor to draw any clear conclusion regarding phase separation. Also, micrographs were not able to show that E-R (5 : 5) is a two-phase blend.

### Compatibility of Rosin and C5-C9 with EVA

The glass transition temperatures of the EVA blends with various proportions of rosin or C5-C9 are shown in Figure 10. The hydrogenated rosin ester is fully compatible with EVA, if the rosin concentration is about 30 wt % or lower. Above 50 wt % of rosin, it is partially compatible with EVA. It is clear that the C5-C9 resin is only partially compatible with EVA, when the C5-C9 concentration is about 30 wt % or higher. This is probably due at least in part to its own heterogeneous nature. However, at 20 wt % of C5-C9, evidence from dynamic testing and TEM was not able to conclude that E-5 (8 : 2) is a two-phase blend.

**Table III** Tan δ Height and Width and Glass Transition Temperature of Various C5-C9-Tackified EVA After Decomposition

EVA	$T_{g-L}$ (°C)	Height	Width (°C)	$T_{g-H}$ (°C)	Height	Width (°C)
E-5 (8 : 2)	-3	.3155	11.2	13	.2092	21.4
E-5 (7 : 3)	-1	.2639	12.4	19	.2974	20.1
E-5 (5 : 5)	9	.2090	18.6	35	.5131	15.1

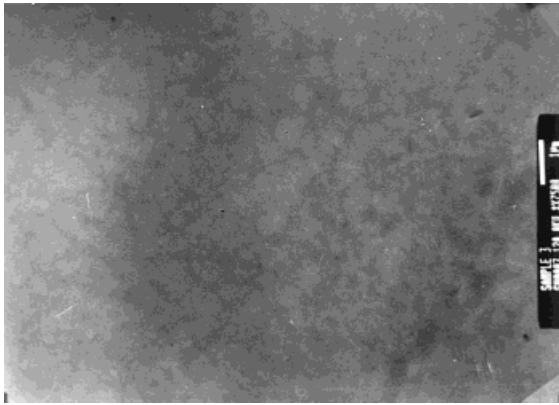


**Figure 7** Morphology observation by the use of TEM for E-5 (7 : 3).

### Comparison Between Viscoelastic Properties of Rosin-Tackified Blends and C5-C9-Tackified Blends

The storage moduli of C5-C9-tackified EVA at concentrations of 30 wt % (Fig. 11) are higher than the corresponding ones for rosin-tackified EVA between  $-10$  and  $25^{\circ}\text{C}$ . Above this temperature range, the opposite is true. When the temperature is above  $25^{\circ}\text{C}$ , both E-5 (7 : 3) and E-R (7 : 3) are in the rubbery state. Therefore, the higher  $E'$  of the rosin-containing adhesives results from the better EVA/rosin compatibility. However, when the temperature is below  $25^{\circ}\text{C}$ , the EVA-rich phases in E-5 (7 : 3) and E-R (7 : 3) are in the rubbery state, while the glassy, resin-rich phase will cause a sharp increase in the storage modulus. Thus, the  $E'$  of E-5 (7 : 3) becomes higher than that of E-R (7 : 3). Below  $0^{\circ}\text{C}$ , the difference in  $E'$  of these two adhesives is within experimental error. A similar trend is observed in the loss moduli of rosin- and C5-C9-tackified EVAs at 30 wt % tackifier.



**Figure 8** Morphology observation by the use of TEM for E-5 (8 : 2).

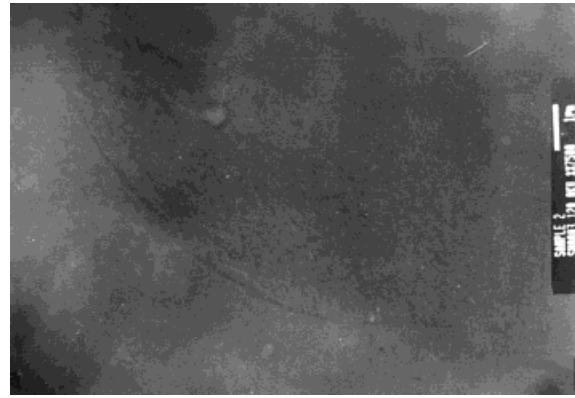


**Figure 9** Morphology observation by the use of TEM for E-R (5 : 5).

E-5 (7 : 3) has a broad  $\tan \delta$  peak (Fig. 4). This results from the poor compatibility between the EVA and C5-C9, noted before. Similar phenomena have been found in plasticized polyvinyl chloride (PVC), which has a broad  $\tan \delta$  peak, when there is poor compatibility between the PVC and the plasticizer.<sup>15</sup>

### T-Peel Strength of E-R (7 : 3) and E-5 (7 : 3)

Strips of PP were bonded with E-R (7 : 3) or E-5 (7 : 3) at  $120^{\circ}\text{C}$  and  $3,400 \text{ kg/m}^2$  for 100 sec. These were tested at 11, 21, and  $31^{\circ}\text{C}$  and at different peeling rates. Results are plotted in Figure 12. Stick-slip failure was observed for both adhesives at  $11^{\circ}\text{C}$ . Adhesives containing rosin always have higher average fracture energies than those of adhesives containing C5-C9.

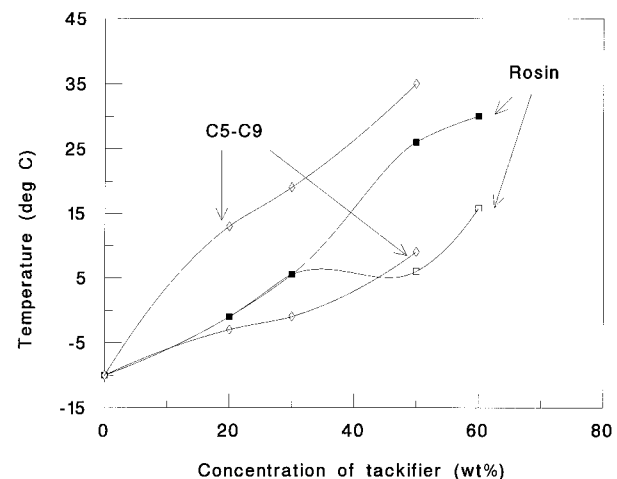


**Figure 10** Effect of rosin concentration on the glass transition temperature of EVA, measured by DMTA at 1 Hz and  $2^{\circ}\text{C}/\text{min}$ .

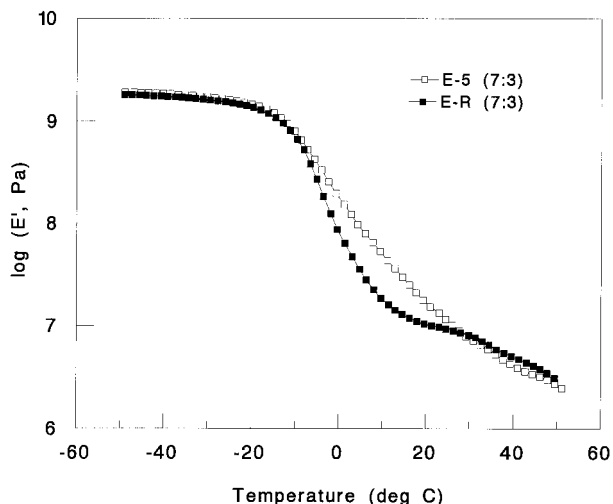


**Figure 11** Effect of tackifier compatibility on the storage modulus of EVA containing 30 wt % of tackifier, measured by DMTA at 1 Hz and 2°C/min.

T-Peel fracture energies at 21°C are plotted against peeling rate in Figure 13. Stick-slip failure was also observed. E-R (7 : 3) has very slightly lower average fracture energies than E-5 (7 : 3), when the peeling rate is lower than 50 mm/min. The reverse is true at peeling rates of more than 50 mm/min.

Figure 14 shows fracture energies at 31°C. Interfacial failure was observed with E-R (7 : 3). However, for E-5 (7 : 3), interfacial failure was only observed for peeling rates lower than 50 mm/min, while stick-slip failure is found at the other two peeling rates.

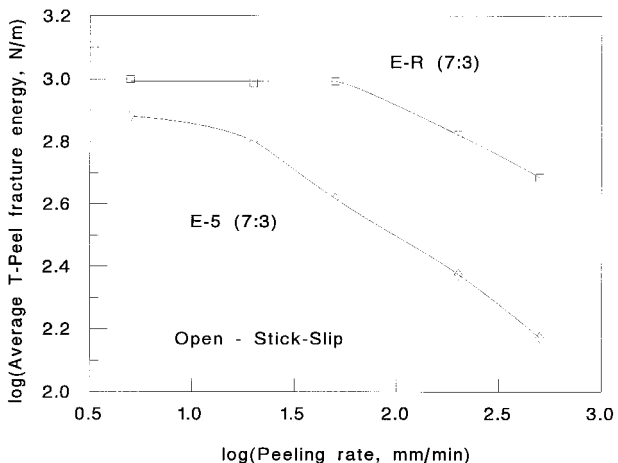


**Figure 12** Average T-Peel fracture energies of PP/HMA/PP, measured at 11°C.

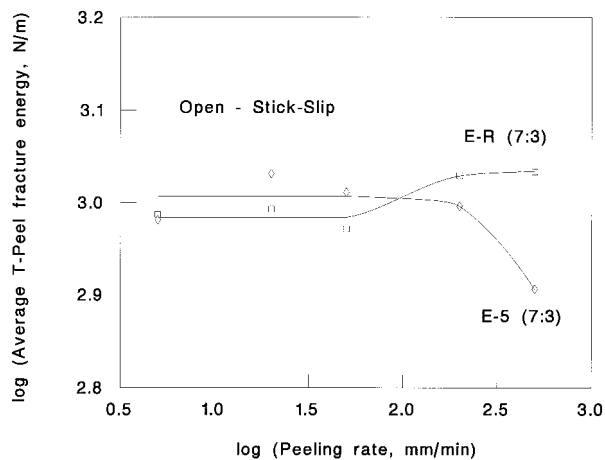


**Figure 13** Average T-Peel fracture energies of PP/HMA/PP, measured at 21°C.

Stick-band fractions are plotted in Figure 15. Values for E-R (7 : 3), tested at 11°C, decrease from 74 to 9% as the peeling rate is increased. Over the same range, stick-band fractions for E-5 (7 : 3) are lowered from 26 to 4%. Stick-band fractions for E-R (7 : 3) at 21°C are higher than 90%, when the peeling rate is lower than 200 mm/min. However, values for E-5 (7 : 3) are within the range of 8% (at 500 mm/min) to 95% (at 5 mm/min). Adhesives containing rosin have higher stick-band fractions than do adhesives containing C5-C9.

### Correlating Viscoelastic Response to T-Peel Strength

There is evidence indicating that E-R (7 : 3) has a more rubbery response than E-5 (7 : 3). First,

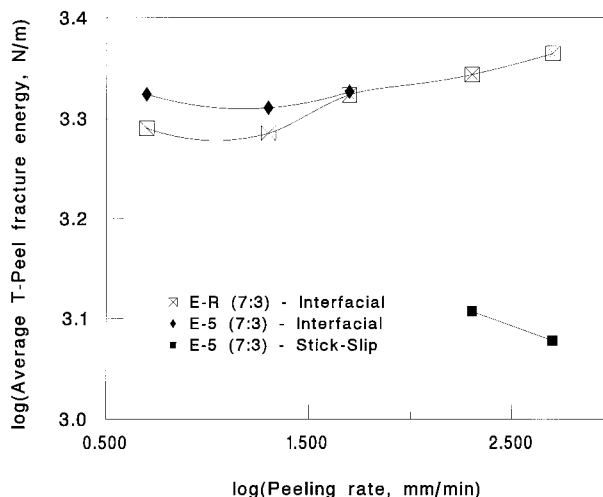


**Figure 14** Average T-Peel fracture energies of PP/HMA/PP, measured at 31°C.

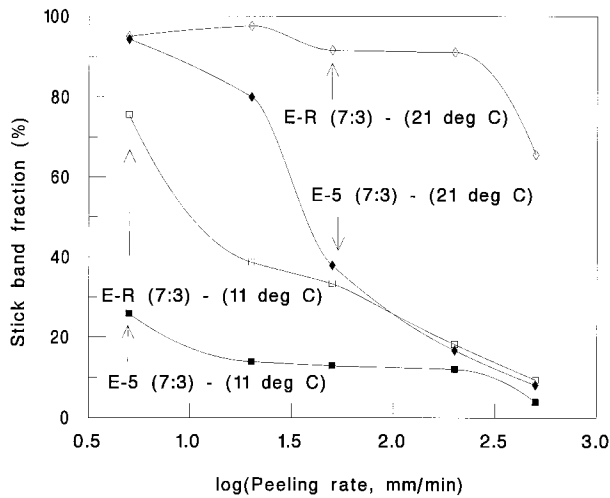


**Figure 15** Stick-band fraction of E-R (7 : 3) and E-5 (7 : 3), tested at 11 and 21°C.

the early appearance of interfacial failure in peel tests for E-R (7 : 3) at 31°C suggests a more glassy response for E-5 (7 : 3) at this temperature. Moreover, at 11, 21, and 31°C, the stick-band fractions for E-R (7 : 3) are higher than those of E-5 (7 : 3). Both findings suggest that E-R (7 : 3) has a more rubbery response than E-5 (7 : 3).

The EVA with 30 wt % rosin has only one glass transition temperature (5.5°C), while the EVA with 30 wt % of C5-C9 has two glass transition temperatures, at -1 and 19°C. At 11°C and a low peeling rate (i.e., 5 mm/min), most of the E-R (7 : 3) has a rubbery response—the stick-band fraction is about 80%. On the other hand, the EVA-rich and C5-C9-rich phases are in the rubbery and glassy states, respectively. This is why E-5 (7 : 3) has a lower stick-band fraction. Thus, the adhesive containing rosin has a more rubbery response. When the temperature is 21°C or higher, the rubbery response of the E-R (7 : 3) and the E-5 (7 : 3) is evident. However, when the peeling rate increases, the rubbery response is reduced, as the adhesive approaches the glassy state. This is why the homogeneous E-R (7 : 3) has a more rubbery response than E-5 (7 : 3), when peeling at 11, 21, and 31°C.

The  $E'$  values of C5-C9-tackified EVA at concentrations of 30 wt % are higher than corresponding ones for rosin-tackified EVA below 25–30°C (Fig. 11). Above this temperature range, the  $E'$  of E-5 (7 : 3) becomes lower than that of E-R (7 : 3). Values are indistinguishable when the temperature is below 0°C. When peeling was conducted at 31°C and low peeling rates, both C5-C9-

and rosin-containing adhesives are in the rubbery state. A higher  $E'$  results in a higher T-Peel strength, as shown in Figure 14. However, stick-slip and interfacial failure were observed at higher peeling rates for E-5 (7 : 3) and E-R (7 : 3), respectively. In this range, E-5 (7 : 3) may have a higher  $E'$  than E-R (7 : 3), which could result in a high T-Peel strength. However, the adhesive containing C5-C9 has a less rubbery response than the one containing rosin, thereby resulting in a lower T-Peel strength. Thus, the T-Peel strength of tackified EVA is compromised by the storage modulus and rubbery response of the adhesive. This explains why the adhesive containing C5-C9 has a lower T-Peel fracture energy at higher peeling rates.

At 21°C, stick-slip failure was observed for both adhesives. At 5 mm/min, the adhesive containing C5-C9 has a similar rubbery response and a slightly higher  $E'$ . This leads to a higher fracture energy for the adhesive containing C5-C9. At a high peeling rate, the stick-band fraction for E-5 (7 : 3) is less than 20%, which is about 60% lower than that for E-R (7 : 3). At the same time,  $E'$  and the stick-band fractions for E-5 (7 : 3) become higher and lower than those for E-R (7 : 3), respectively. These opposing effects result in a small difference in the T-Peel fracture energy between E-5 (5 : 5) and E-R (5 : 5).

When test temperature decreases to 11°C, stick-slip was observed. E-5 (7 : 3) has a slightly higher storage modulus than E-R (7 : 3) at lower peeling rates.  $E'$  becomes equal as the peeling rate is increased. The stick-band fraction of E-5 (7 : 3) is quite low, indicating a more glassy response. Thus, the adhesive containing C5-C9 has a lower T-Peel fracture energy.

## SUMMARY

Rosin tackifier is fully compatible with EVA at concentrations below 30 wt % but becomes partially compatible with EVA when this concentration is exceeded. C5-C9 tackifier is heterogeneous, resulting in partial compatibility with EVA.

EVA/rosin adhesives have higher storage and loss moduli than does the EVA/C5-C9 mixture, when the adhesives are in the rubbery or glassy state. However, the reverse is true when the temperature is between the glass transition temperatures of the EVA- and tackifier-rich phases of the C5-C9/EVA blends. This results from the glassy



C5-C9-rich phase, which acts as a reinforcing filler.

The T-Peel strength of tackified EVA is controlled by the viscoelastic response, i.e., the storage modulus and the degree of rubbery response. A higher T-Peel strength results from a higher  $E'$  and a more rubbery response. For a heterogeneous EVA blend, the glassy, tackifier-rich phase increases the storage modulus, when temperature approaches the glass transition temperature of this phase. The increase in storage modulus enhances peel strength. For example, at 21 and 31°C at a low peeling rate, a heterogeneous adhesive has a higher T-Peel strength than does a homogeneous one. In other words, a poorly compatible EVA/tackifier blend can have a higher T-Peel strength than does a composition with a more compatible tackifier, under certain conditions.

One of the authors (H.-H.S.) gratefully acknowledges the Industry Technology Research Institute (ITRI), Taiwan, R.O.C., for the continuous financial support during his study at the University of Akron. The authors also thank the Exxon and Hercules companies for their support. Many thanks go to Mr. Chung-Sea Shen for his help in decomposition software and to Mr. Rong-Ming Ho as well as Miss Su-May Wei for their help in TEM observations.

## REFERENCES

1. E. F. Eastman and L. Fullhart, Jr., in *Handbook of Adhesives*, I. Skeist, Ed., Van Nostrand Reinhold, New York, 1990.
2. G. R. Hamed, *Rubber Chem. Technol.*, **54**, 576 (1983).
3. M. F. Tse, *J. Adhes. Sci. Technol.*, **3**, 551 (1989).
4. J. B. Class and S. G. Chu, *J. Appl. Polym. Sci.*, **30**, 805 (1985).
5. J. B. Class and S. G. Chu, *J. Appl. Polym. Sci.*, **30**, 815 (1985).
6. J. B. Class and S. G. Chu, *J. Appl. Polym. Sci.*, **30**, 825 (1985).
7. M. F. Tse, L. Hendewerk, K. O. McElrath, and M. Faissat, *The Adhesion Society Proceedings of the Fourteenth Annual Meeting*, 161-3.9(12)4, 1991.
8. A. S. Tathgur, thesis, University of Akron, Akron, Ohio, 1991.
9. M. Sherriff, R. W. Knibbs, and P. G. Langley, *J. Appl. Polym. Sci.*, **17**, 3423 (1973).
10. G. Kraus and T. Hanshimoto, *J. Appl. Polym. Sci.*, **27**, 1745 (1982).
11. L. C. Sawyer and D. T. Grubb, *Polymer Microscopy*, Chapman and Hall, New York, 1987.
12. I. A. Schlademan, in *Handbook of Pressure Sensitive Technology*, D. Statas, Ed., Van Nostrand Reinhold, New York, 1989.
13. J. F. Holohan, Jr., J. Y. Penn, and W. A. Vredenburg, in *Encyclopedia of Chemical Technology*, Vol. 12, H. F. Mark, D. F. Othmer, C. G. Overberger, and G. T. Seaborg, Eds., John Wiley & Sons, Inc., New York, 1983.
14. A. H. Warth, *The Chemistry and Technology of Wax*, Reinhold Publishing Corporation, New York, 1956.
15. L. E. Nielsen, *Mechanical Properties of Polymers and Composites*, Vol. 1, Marcel Dekker, New York, 1974.

Received March 13, 1996

Accepted July 27, 1996